MAGNETIC RESONANCE IN MEDICINE 12, 99–113 (1989)

Compensation for Effects of Linear Motion in MR Imaging

HOPE W. KORIN,* FARHAD FARZANEH,* RONALD C. WRIGHT,*
AND STEPHEN J. RIEDERER

Department of Diagnostic Radiology, Mayo Clinic, Rochester, Minnesota 55905

Received July 13, 1988; revised December 15, 1988

Various compensation methods for different types of motion during MR image acquisition have been proposed. Presented here is a postprocessing scheme for eliminating artifacts due to linear, intra-slice motion of known velocity. The data for each phase encoding or "view" acquired from a moving object are shown to differ from those which would be measured from the stationary object by a phase factor which depends on the object's displacement from a reference point. This derivation is then used to propose a correction scheme for linear motion in which all phase encodings measured at different positions of the moving object are collapsed onto the same reference position. After subsequent reconstruction, the object appears perfectly "focused." By selection of different reference positions, the method permits positioning of the compensated object as desired within the field of view of the image. This property allows the method to be extended to create sequences of corrected images with smooth object motion between frames of the sequence. The basic correction scheme and its variations were tested experimentally in phantom studies with velocities as large as 8 cm/s.

INTRODUCTION

Motion of a subject during MR image acquisition causes major artifacts in the reconstructed images. It is a challenge not only to compensate for or eliminate such artifacts but also to categorize and explain them in the first place. For standard two-dimensional Fourier transform (2DFT) imaging (*1, 2*) various methods of compensation have been devised. These include reordering the acquisition of the phase encodings to address the problems of respiratory motion (*3*) and gradient moment nulling to ensure that moving spins are not dephased (*4, 5*).

The problem we wish to address in this work is that of correction for linear, intra-slice motion which can occur throughout the duration of a scan. Before discussing this in detail, however, we wish to differentiate between two classes of inconsistencies in the acquired data, both of which are due to motion and both of which cause artifacts in the reconstructed images. As in the distinction made by Pattany *et al.* (*4*), we call these "intra-view" and "inter-view" effects. Here the term view refers to the process of the measurement of a single phase encoding. Intra-view inconsistency is caused by motion of an object in the interval between the initial RF pulse and the readout of the echo. A common example is the in-plane motion of blood with a range of velocities. Because of velocity dispersion, there will be a difference in the net

* Also of the Department of Radiology, Duke University Medical Center, Durham, NC 27710.

0740-3194/89 $3.00

accumulation of phase by spins moving at different velocities, and upon reconstruction some blood signals will be reconstructed at only a fraction of their ideal value. Because of the manner in which the frequency-encoding gradients are applied, this phenomenon is eliminated in the second echo of a two-echo spin-echo sequence (*6*) if equal temporal spacing between echoes is chosen. Another example of intra-view inconsistency is the misplacement of objects in the image due to motion which occurs between the phase-encoding and the readout gradients (*7*). Such effects can be reduced in severity if the total time spanned by the gradient signals is minimized; i.e., if the phase encoding, for example, is applied immediately before the signal readout (*8*). Phase problems are compounded if the net phase accumulation differs from view to view, such as if pulsatile blood flow occurs during a scan (*9*). However, the problem of differential phase accumulation can be substantially eliminated with gradient moment nulling (*4, 5*), which ensures that spins moving with linear or higher order motion have zero net phase at the first echo.

Inter-view effects are taken to be inconsistencies due to motion between views. A paradigm is respiratory motion which, if uncorrected, leads to ghosting in the phase-encoded direction (*10*). A reordering of the acquisition of the phase encodings using ROPE (*3, 11*) or Exorcist techniques can suppress the ghosts, but this does not eliminate blurring.

In this manuscript, we consider another inter-view effect, that of linear motion within the image slice with velocity of known direction and magnitude. Because the object is moving, its position is different from view to view. Thus, this situation is distinct from the blood velocity case mentioned above in which differential phase is accumulated within a view. The situation addressed here is an inter-view inconsistency while gradient moment nulling addresses an intra-view inconsistency.

An investigation into the mathematics of this situation not only produces an explanation for the motion artifacts observed but also reveals a method of compensation by postprocessing of the acquired image data. This compensation scheme can generate a corrected image of the object where the exact position to which it is reconstructed within the field of view can be chosen as desired. Moreover, as we will show, it becomes possible to generate a continuous sequence of focused images of the moving object.

Clinically, this scheme would be useful in imaging any object which moves within the slice during a scan. In particular, it could be used in conjunction with a fast-scanning sequence such as MR fluoroscopy (*12*) to produce images of high enough quality to enable localization of structures in real time during patient positioning. In this case the patient table could be translated through the gantry with a velocity under operator control. Further, the scheme presented here can potentially be extended to the important physiological case in which the in-slice motion is nonlinear. We discuss how such a scheme could be implemented under Discussion.

In the following sections, we present the theory for signal alteration due to linear motion, a compensation scheme for it, and experimental results. The experiments presented consist of correction of single images and generation of continuous image sequences of the moving object. The latter incorporates both correction for motion artifacts and selective placement of the object within the field of view.

THEORY

The MR signal measured during a standard spin-warp image acquisition can be described by (*1, 2*)

$$s_n(t) = \iint m(x, y)e^{-i\gamma G_n y t_y}e^{-i\gamma G_x x t}dxdy, \qquad [1]$$

where x is the frequency-encoding (or readout) direction, y is the phase-encoding direction, G_x and G_n are the respective gradients, $m(x, y)$ is the transverse magnetization of the object in spatial coordinates, γ is the gyromagnetic ratio, and t_y is the duration of the y gradient. n is an index over the repetition number of the acquisition. It runs from 0 to $N - 1$, where N is the total number of phase encodings.

If we consider an object moving in the plane of the selected slice, we can describe its velocity by two orthogonal components, v_x and v_y, in the frequency and phase directions. Its position in the x and y coordinates at the time of the measurement of the signal can then be described as $(x_0 - v_x t_n, y_0 - v_y t_n)$, where t_n is the time of measurement of the nth phase encoding and x_0 and y_0 describe an arbitrary reference position. $v_x t_n$ and $v_y t_n$ are the displacements of the object from this original reference. We are ignoring the time delays due to the digitization during each signal measurement because they are very much smaller than those due to the repetition times between acquisition of different signals. Translating this into mathematics and inserting it into Eq. [1] gives a formula for the signal $s'_n(t)$ measured for the case of motion:

$$s'_n(t) = \iint m(x - v_x t_n, y - v_y t_n)e^{-i\gamma G_n y t_y}e^{-i\gamma G_x x t}dxdy. \qquad [2]$$

Now, using the substitution of variables

$$\xi = x - v_x t_n \qquad [3a]$$

$$\eta = y - v_y t_n \qquad [3b]$$

we find

$$s'_n(t) = \iint m(\xi, \eta)e^{-i\gamma G_n(\eta + v_y t_n)t_y}e^{-i\gamma G_x(\xi + v_x t_n)t}d\xi d\eta \qquad [4a]$$

$$= \iint m(\xi, \eta)e^{-i\gamma G_n \eta t_y}e^{-i\gamma G_n v_y t_n t_y}e^{-i\gamma G_x \xi t}e^{-i\gamma G_x v_x t_n t}d\xi d\eta \qquad [4b]$$

$$= e^{-i\gamma G_n v_y t_n t_y}e^{-i\gamma G_x v_x t_n t}\iint m(\xi, \eta)e^{-i\gamma G_n \eta t_y}e^{-i\gamma G_x \xi t}d\xi d\eta \qquad [4c]$$

$$= e^{-i\gamma G_n v_y t_n t_y}e^{-i\gamma G_x v_x t_n t}s_n(t), \qquad [4d]$$

where the last result follows from Eq. [1].

We note that $s'_n(t)$, the signal measured from the moving object, is simply $s_n(t)$, the signal from the stationary object measured for that phase encoding, multiplied by a phase factor which depends on the velocity of the object and the time at which the signal was measured. In other words, the phase factor depends on the displacement of the object at the time of the measurement from some arbitrary reference point.

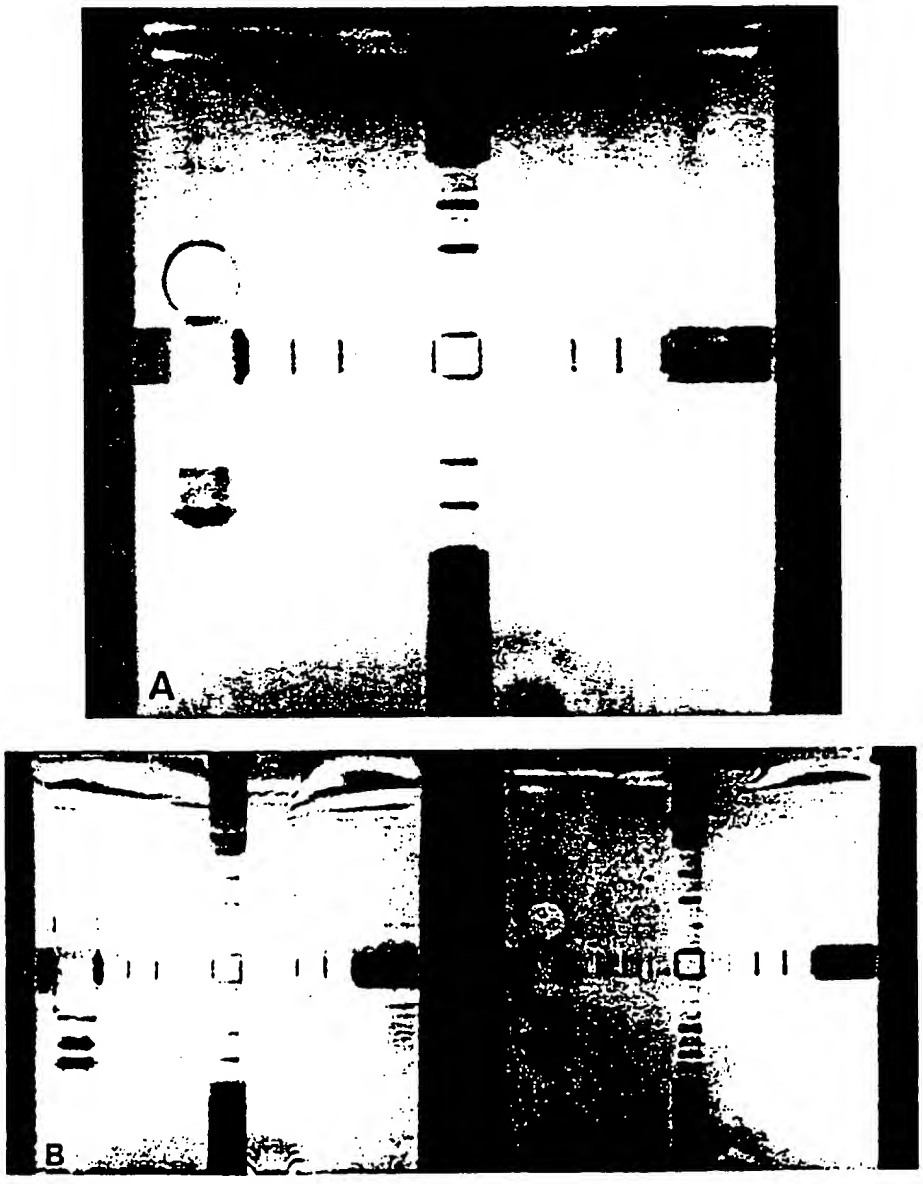

FIG. 1. Motion in the phase-encoded direction (uncompensated images on the left, compensated on the right): (A) static phantom. (B) velocity of 1 cm/s. (C) 2 cm/s. (D) 4.2 cm/s. and (E) 8.4 cm/s. The two white bars in (E) indicate the distance traveled by the phantom during image acquisition. The motion was in the upward direction.

Rather than work with Eq. [4d] in its present form with its explicit dependence on the values of the gradients, we note that the phase factors can be converted to field of view (FOV) dependence as follows.

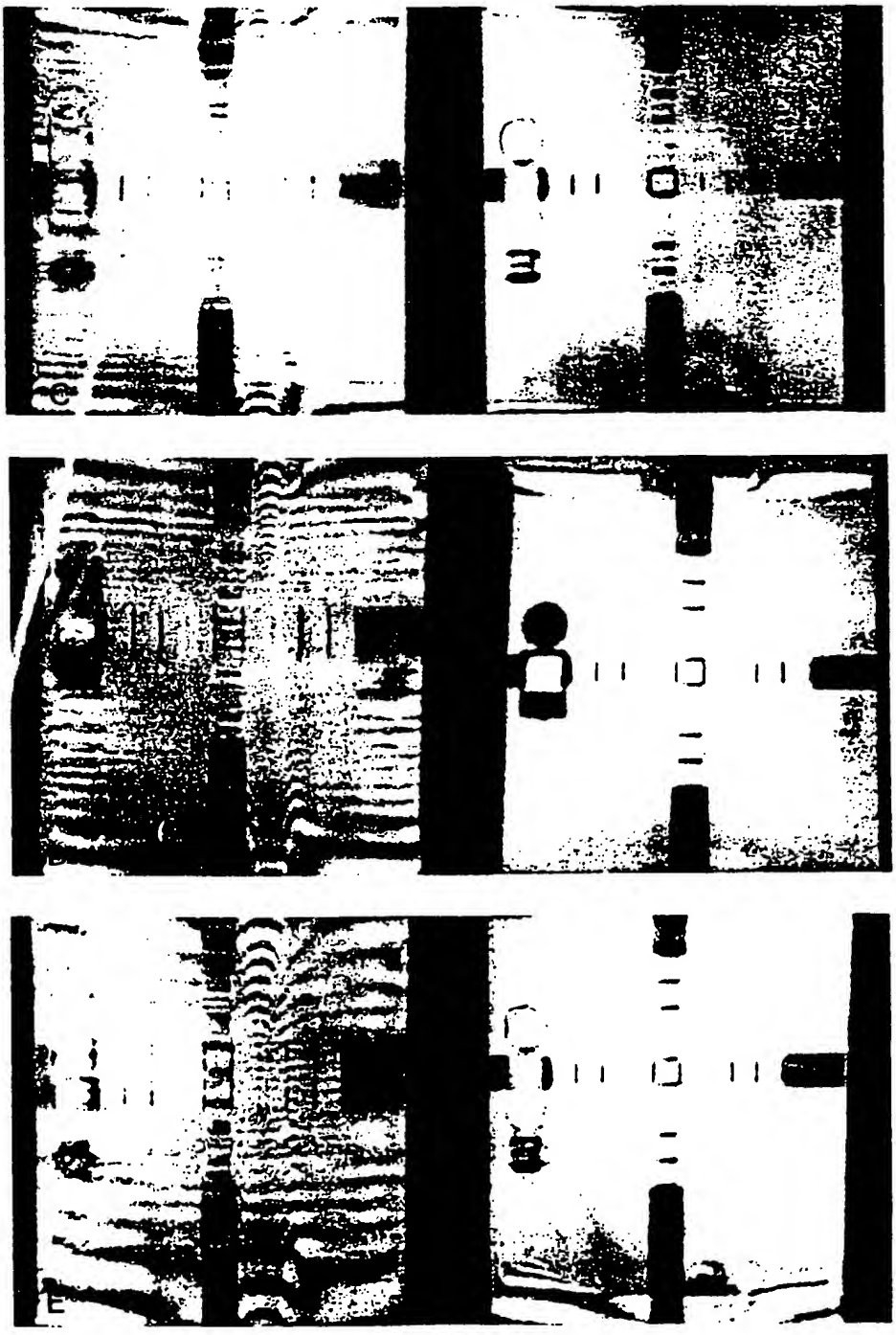

FIG. 1—*Continued*

If the phase encodings (views) are applied in a standard sequential manner, then we have

$$G_n = \left(n - \frac{N-1}{2}\right)\Delta G_y. \quad [5]$$

Recall that N is the total number of views per image and n is an index over these views, running from 0 to $N-1$. ΔG_y is the incremental change in the encoding gradient from view to view. In general, ΔG_y is related to the field of view (FOV) by (2)

$$\Delta G_y = \frac{2\pi}{\gamma t_y(\mathrm{FOV})}. \quad [6]$$

Therefore, the first phase factor of Eq. [4d] can be rewritten as

$$e^{-i2\pi(n-(N-1)/2)y_i t_n/\mathrm{FOV}}. \quad [7]$$

Similarly, the gradient in the x (readout) direction can be written as

$$G_x = \frac{2\pi}{\gamma \Delta t(\mathrm{FOV})}, \quad [8]$$

where Δt is the interval between the samples taken of the MR signals and we have assumed the same FOV in x as that in y. We next note that t for the readout direction is equal to zero at the center of the echo signal.

$$t = \left(m - \frac{M-1}{2}\right)\Delta t, \quad [9]$$

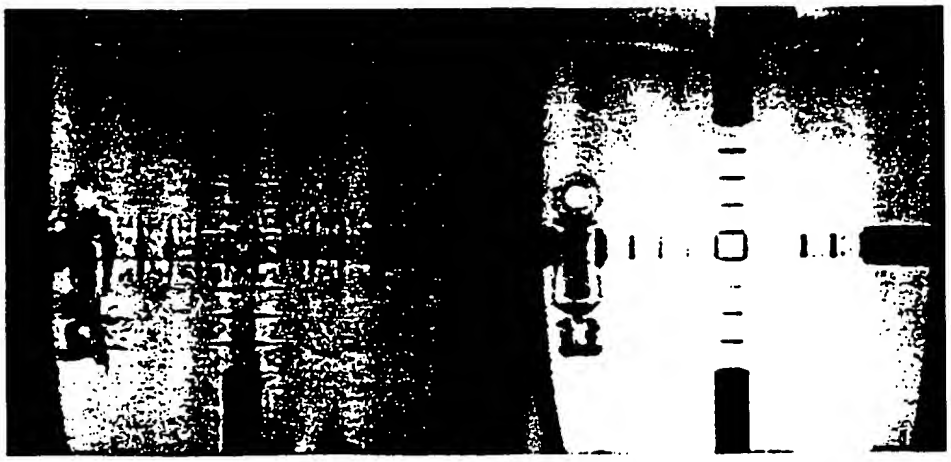

FIG. 2. Motion in the frequency-encoded direction (uncompensated image on the left, compensated on the right), velocity of 1 cm/s. The motion was in the upward direction.

FIG. 3. Comparison of two compensated images in which the phantom moved an equal distance during the image acquisition time. The image on the left was acquired with a velocity of 1 cm/s, TR of 35 ms, that on the right with a velocity of 2 cm/s, TR of 17.5 ms.

where m is the index of the readout point and M is the total number of readout points, similar to n and N in the phase-encoding direction. We can then rewrite Eq. [4d] as

$$s'_n(t) = e^{-i2\pi(n-(N-1)/2)v_y t_n/\mathrm{FOV}} e^{-i2\pi(m-(M-1)/2)v_x t_n/\mathrm{FOV}} s_n(t). \quad [10]$$

This is the equivalent of Eq. [4d], but with the FOV rather than gradient dependence within the phase factors.

It is thus apparent from Eq. [10] that it is possible to recover the signal of the stationary object by multiplying the data from the moving object by the inverse of these phase factors, namely

$$s_n(t) = e^{+i2\pi(n-(N-1)/2)v_y t_n/\mathrm{FOV}} e^{+i2\pi(m-(M-1)/2)v_x t_n/\mathrm{FOV}} s'_n(t). \quad [11]$$

This is the basic correction scheme. For the cases of separate motion in either the frequency or phase-encoding direction, Eq. [11] simplifies because v_x and v_y are respectively zero in these cases.

In Eq. [11], vt_n, as previously discussed, represents the displacement of the object from its stationary position. This displacement will be different for every view acquired, as the object moves a distance vTR between each two consecutive views. Multiplying each phase encoding by its specific phase factor in essence collapses all of them onto the position chosen as the stationary reference. It is thus possible to create images of the object from the same data set in which the object is centered at different locations within the field of view simply by choosing different reference positions for it.

EXPERIMENTAL RESULTS

Single Images

The compensation technique of Eq. [11] was implemented experimentally on a GE Signa MR system. A limited flip angle pulse sequence (*13*) with the "GRASS"

FIG. 4. Illustration of object positioning. In (A), the reference view is −64; in (B), the reference view is +63. Both images were generated from the same image data. Note the difference in object position.

variation (*14*) was used with TR/TE values of 17.5/8.9 ms and a field of view of 24 cm. The object was moved by placing it on a table and translating the table through the gantry at an operator-controlled speed. A slice transecting the end of the phantom and parallel to the tabletop was imaged. By adjusting the pulse sequence, phase or frequency encoding was applied in the direction of the motion as desired. One hundred twenty-eight phase encodings were applied sequentially from most negative to most positive and then repeated.

$$-64, -63, \ldots, -1, 0, +1, \ldots, +63, -64', -63', \ldots,$$

the prime indicating the second application of a given encoding. Images were reconstructed from 128 consecutive views, and successive images were displaced by 32 encodings. That is, Image 1 was formed from views −64 to +63, Image 2 from −48

FIG. 4—*Continued*

to +63, and −64′ to −49′, etc. This is in essence the MR fluoroscopy reconstruction described in Ref. (*12*).

The first study is presented in Figs. 1 to 3. Figure 1 shows an image of the stationary object (A), as well as uncompensated and compensated images of the object moving in the phase-encoded direction at speeds of 1 (B), 2 (C), 4(D), and 8 (E) cm/s. In all the images shown, the motion was in the upward direction. Figure 1D shows a slightly different slice through the phantom than the other images. In Fig. 1E, the two white lines at the top and near the bottom of the compensated image indicate the extremes of the distance traveled by the crossbar of the phantom during the acquisition of the 128 views necessary to create the image. Figure 2 shows uncompensated and compensated images of the object moving in the frequency-encoded direction at a speed of 1 cm/s. Again the motion was upward. It is interesting to note the difference in the appearance of the artifacts between motion in the frequency-encoded

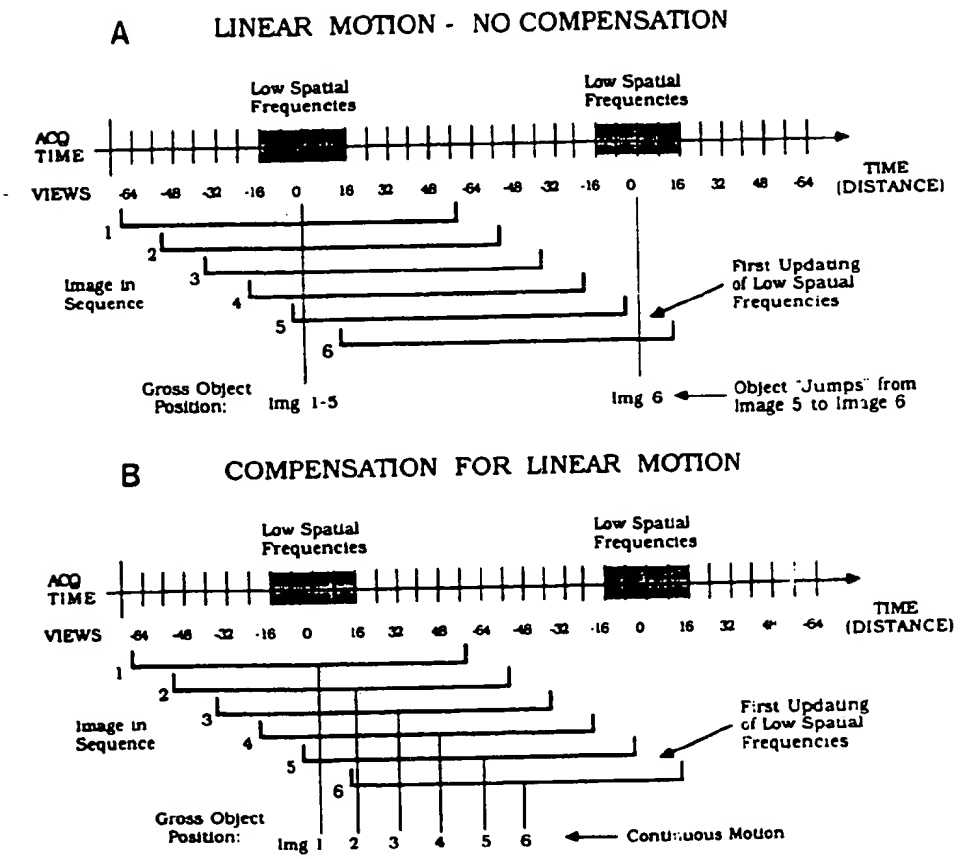

FIG. 5. Schematic of creation of image sequences with MR fluoroscopy. (A) Object position with no compensation scheme implemented. (B) continuous motion possible with compensation.

direction (Fig. 2, left) and phase-encoded direction (Figs. 1B–1E, left). The slight curvature of the periphery of the image is due to spatial distortion caused by gradient nonlinearity. However, this does not affect the focusing of the image. Figure 3 is a comparison of two compensated images in which the phantom moved an equal distance during the image acquisition time. The image on the left was acquired with a velocity of 1 cm/s and a TR of 35 ms, and that on the right with a velocity of 2 cm/s and a TR of 17.5 ms. That is, in each case the incremental displacement between successive phase encodings was vTR or 0.35 mm. As expected, the quality of the two images is very similar. The pattern of the artifacts in the uncompensated images (not shown) is also similar.

In all the images of Figs. 1 to 3, the middle of the time interval of data acquisition for the image was chosen as the reference position for the object. As can be seen, each of the compensated images is of quality comparable to that of the stationary image (Fig. 1A).

The second study involved investigating the modification of a single data set to generate images with various object positions. A series of images was created, all from

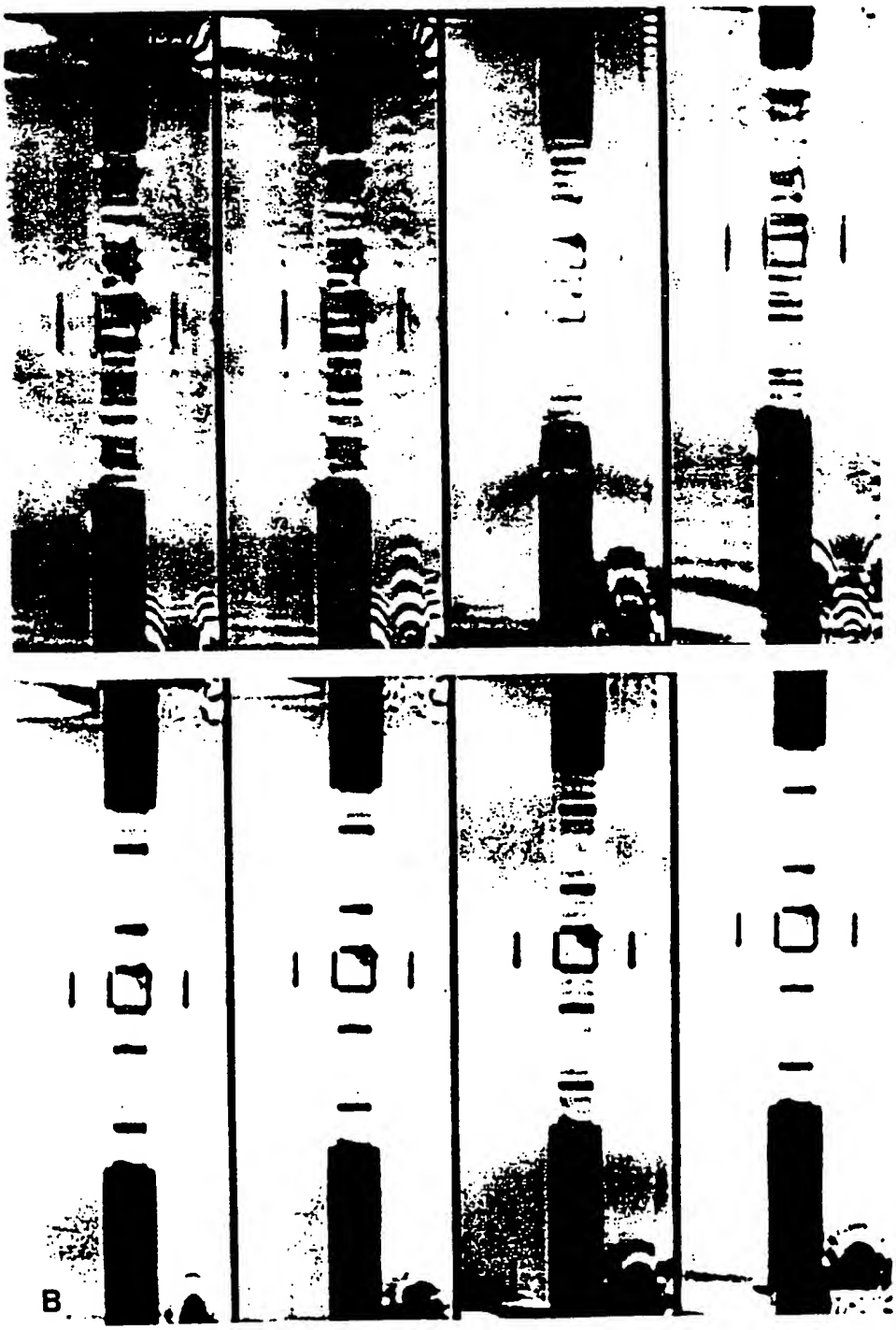

FIG. 6. Stills of an image sequence. The middle section of four frames from the sequence is shown. (A) The uncompensated images, (B) the compensated ones. Note the even motion between the compensated panels, as opposed to the "jumps" between the panels of (A), and the improvement in image clarity.

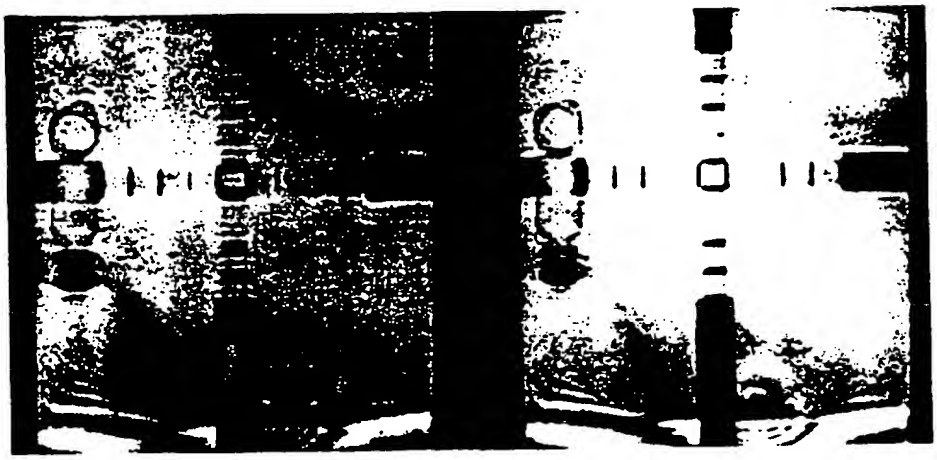

FIG. 7. Illustration of velocity tuning. The actual velocity was 8.4 cm/s, shown on the right. The image on the left shows the effect of implementing the compensation scheme on these data assuming the incorrect velocity of 8.2 cm/s.

the same data set of 128 views (numbered −64 to +63), such that in each image the measurement time of a different phase encoding was selected as the reference point. This is equivalent to choosing the time at which the reference phase encoding was measured to be the zero of the time scale. Figure 4 shows two of these compensated images generated from the same data set with phantom motion of 1 cm/s in the phase-encoding direction. In Fig. 4A, the reference view is −64, the first encoding of 128 acquired. That is, although each view was measured with a different object position, each was multiplied by the appropriate phase factor to shift its object position back to that measured by the −64 view. In Fig. 4B, the reference encoding is +63, the last one measured. Here the views are collapsed forward onto it. The difference in position of the object between the two images is easily seen.

Image Sequences

This technique is of great interest for application to MR fluoroscopy imaging (*12*). Fluoroscopy is a fast-scanning technique that seeks to produce images of dynamic systems in real time, such as in patient positioning before a scan. In this case, a sequence of corrected images of the moving object would be desirable to produce a video sequence of the motion. The two main undesirable effects observed in uncompensated videos of moving objects are the motion artifacts themselves and the large "hops" or "jumps" of object position seen instead of continuous motion between video frames (*12*). In some frames, a duplication of the object is even observed. An explanation for the large hopping movements and the object duplication is shown in Fig. 5A. This figure is a plot versus time of the application of phase encodings. One can also imagine for purposes of discussion that the object is moving to the right. Two repetitions of the application of 128 views are shown, as discussed previously. Images are formed by taking a set of 128 contiguous phase encodings. Here the offset

between successive images is chosen to be 16 views for illustrative purposes. The low spatial frequencies represent the encoding of the gross position of the object. Higher frequencies represent the edges. Let us assume initially that no motion compensation is done. Then Images 1 through 4 will show the gross object position to be the same since they all use the same low-frequency measurements in their reconstruction. It is the edges of the object which will be updated in going from Image 1 to 4 and in fact, the edges of the object appear to move ahead of the object. Image 5 will show the effect of duplication of the object because it incorporates low spatial frequency measurements from two distinct times and thus two distinct object positions. Image 6 will show the second gross position of the object only and so forth. Because the gross position of the object will change only when a new set of low frequencies is measured, it appears to be stationary for a number of images (4 or 5 in this illustration) and then will hop a considerable distance on the next image.

It is possible to eliminate these effects by applying the features of the correction scheme discussed previously under single image compensation. This is illustrated in Fig. 5B. By implementing the correction method, not only are the motion artifacts eliminated, but also the hopping motion is eradicated by a judicious choice of the reference position of the object in each image. If we choose the position of the object at the center of the data acquisition time to be the reference position of the object (i.e., view 0 in Image 1, view 16 in Image 2, and view 32 in Image 3) we can generate a sequence of images of the moving object in which the distance traveled by the object between successive frames is always the same; thus a clear, continuously moving object is seen.

Figures 6A and 6B show stills of such an image sequence. This sequence was reconstructed with a displacement between images of 32 views instead of the 16 shown in the drawings of Fig. 5, but the principle is the same. The center portions of four uncompensated images from the sequence are shown in (A), the corresponding compensated ones in (B). It should be stressed that the same data set was used for each sequence. Image 1 (panel 1 in (B), numbering the panels from left to right) was compensated to view 0, Image 2 (panel 2) to view 32, Image 3 (panel 3) to view −64, and Image 4 (panel 4) to view −32. Note the apparent continuous motion of focused images in (B) as opposed to the hopping motion in the uncompensated images of (A) and the elimination of the duplication of the object in panel 3.

DISCUSSION

In the work presented here, we have described how the signals acquired during a spin-warp pulse sequence are modified if an object moving at constant, linear velocity within the slice is imaged. It was shown that such signals differ from the signal that would be acquired from a stationary object by a phase factor, different for each view and dependent on the distance the object has traveled from some reference position. It is thus possible to generate an uncorrupted image of the object by multiplying the data acquired by the inverse of these phase factors. Moreover, as there is no predefined reference position, it is possible to choose it as desired, and thus position the object arbitrarily within the field of view during the postprocessing scheme.

Because the experiments described here were performed with a moving phantom, one might question whether there were any intra-view inconsistencies in the acquired

data. Because the *entire* object was moving at the *same* velocity, the accumulated phase of all spins within a single view was identical. Additionally, because the velocity was nominally constant throughout the entire scan, this phase accumulation was the same for every view. Hence, there were no inconsistencies due to intra-view motion. The effects were solely due, as desired, to different view-to-view displacements of the object from a reference position.

The basic correction scheme was verified experimentally with velocities as high as 8 cm/s. At this speed, the object movement during acquisition of all the views necessary to reconstruct one image was about 75% of the field of view. The modified technique of object placement within the field of view was also investigated. Both methods were then used to generate sequences of images in which the motion from one video frame to the next was not only free of artifacts, but also displayed smooth and continuous motion.

A potential extension to this method is velocity tuning, in which the operator could retrospectively determine the velocity at which an object was traveling by adjusting the phase factors until the images cleared. An example of implementing the correction scheme with a slightly incorrect velocity is shown in Fig. 7. The image on the left was reconstructed assuming a velocity of 8.2 cm/s, instead of the correct 8.4 cm/s shown on the right. Note especially the focusing of the lines in the vertical crossbar of the phantom. Clearly, if one attempts to image a collection of objects which are moving at different rates, this method alone would not permit focusing of all of them at once. Also, parts of the object entering the slice for the first time may not be corrected properly.

In the derivation and experimental results described here, we assumed the special case of linear motion with known velocity. Other than the MR fluoroscopy/moving table example mentioned earlier, one may question how this can relate to clinical imaging. In fact, the derivation and correction can easily be modified to allow for a more general case. Suppose in the nth view that the displacement of the object of interest from a reference position is some arbitrary x_n rather than the $v_x t_n$ assumed in Eq. [2]. In this case, it is straightforward to show that the same substitution (x_n for $v_x t_n$) is made in the correction term of Eq. [4d]. Having derived this, one next questions how the set of displacements $\{x_n\}$ can be measured. In fact this can be readily accomplished using a dual-echo pulse sequence in which one echo encodes the desired image information and the second echo (a "monitor" or "navigator" echo at the zeroth phase encoding) is used to monitor the view-to-view displacements of a potentially moving structure (*15*). This concept of using a navigator echo in conjunction with the data correction scheme presented in this work has been proposed by Ehman *et al.* (*16*). It is expected that such a technique can more completely correct clinical images for motion blurring than present methods.

ACKNOWLEDGMENTS

We acknowledge the support of National Institutes of Health Grant CA37993 awarded by the Public Health Service and of General Electric Medical Systems.

REFERENCES

1. A. KUMAR, D. WELTI, AND R. R. ERNST, *J. Magn. Reson.* **18**, 69 (1975).
2. W. A. EDELSTEIN, J. M. S. HUTCHISON, G. JOHNSON, AND T. REDPATH, *Phys. Med Biol.* **25**, 751 (1980).

3. D. R. Bailes, D. J. Gilderdale, G. M. Bydder, A. G. Collins, and D. N. Firmin, *J. Comput. Assist. Tomogr.* **9**, 835 (1985).
4. P. M. Pattany, J. J. Phillips, L. C. Chiu, J. D. Lipcamon, J. L. Duerk, J. M. McNally, and S. N. Mohapatra, *J. Comput. Assist. Tomogr.* **11**, 369 (1987).
5. E. M. Haacke and G. W. Lenz, *Amer. J. Roentgenol.* **148**, 1251 (1987).
6. V. Waluch and W. G. Bradley, *J. Comput. Assist. Tomogr.* **8**, 594 (1984).
7. R. L. Ehman, M. T. McNamara, R. C. Brasch, J. P. Felmlee, J. E. Gray, and C. B. Higgins, *Radiology* **159**, 777 (1986).
8. P. M. Joseph, A. Shetty, and E. A. Bonaroti, *Med. Phys.* **14**, 608 (1987).
9. W. H. Perman, P. R. Moran, R. A. Moran, and M. A. Bernstein, *J. Comput. Assist. Tomogr.* **10**, 473 (1986).
10. M. L. Wood and R. M. Henkelman, *Med. Phys.* **12**, 143 (1985).
11. M. L. Wood and R. M. Henkelman, *Med. Phys.* **13**, 794 (1986).
12. S. J. Riederer, T. A. Tasciyan, J. N. Lee, R. C. Wright, F. Farzaneh, and R. J. Herfkens, *Magn. Reson. Med.* **8**, 1 (1988).
13. J. Frahm, A. Haase, and D. Matthael, *Magn. Reson. Med.* **3**, 321 (1986).
14. J. A. Utz, R. J. Herfkens, J. A. Heinsimer, T. Bashore, R. Califf, G. Glover, N. Pelc, and A. Shimakawa, *Amer. J. Roentgenol.* **148**, 839 (1985).
15. R. S. Hinks, "Monitored Echo Gating for the Reduction of Motion Induced Errors in T2-Weighted MRI," presented at the 6th Annu. Meet. Soc. Magn. Reson. Imaging, Boston, March 1988.
16. R. L. Ehman, J. P. Felmlee, R. L. Morin, and J. E. Gray, "Comprehensive Method for Reducing Physiologic Motion Artifact in MR Imaging," presented at the 74th Annu. Meet. Radiol. Soc. North Amer., Chicago, November 1988.